Chemical Engineering Journal, Volume 408, March 2021, Article number 127322
DOI:10.1016/j.cej.2020.127322

Mechanisms of genuine humic acid evolution and its dynamic interaction with methane production in anaerobic digestion processes

Xiqing Wang[1], Atif Muhmood[1], Tao Lyu[2], Renjie Dong[1], Hongtao Liu[3], Shubiao Wu [*4]

[1] *Key Laboratory of Clean Utilization Technology for Renewable Energy, Ministry of Agriculture, College of Engineering, China Agricultural University, 100083, Beijing, P. R. China*

[2] *Cranfield Water Science Institute, Cranfield University, College Road, Cranfield, Bedfordshire, MK43 0AL, UK*

[3] *Institute of Geographic Science and Natural Resources Research, Chinese Academy of Sciences, Beijing 100101, China*

[4]*Aarhus Institute of Advanced Studies, Aarhus University, DK-8000 Aarhus C, Denmark*

*Correspondence. E-mail: wushubiao@gmail.com

Abstract

Humic acid (HA), a byproduct formed during the biological conversion of organic matter into biogas in the anaerobic digestion (AD) process, contains complex structures and redox functions. However, the evolution mechanism of HA and its interaction with CH_4 production during the AD process have not been fully explored, particularly with respect to various substrates and temperature conditions. In this study, we investigated the evolutionary dynamics of the structure and function of genuine HA that naturally formed in the AD processes of chicken manure and corn stover under mesophilic (37 °C) and thermophilic (55 °C) conditions. The results demonstrated that the HA evolution mechanisms in AD of chicken manure and corn stover have different pathways. The AD of core stover showed higher degree of aromaticity (41.2-66.7% and 45.3-68.4% for mesophilic and thermophilic respectively) and humification index (1.5-4.2 and 2.8-4.5 for mesophilic and thermophilic respectively) than those (28.3-45.3% and 30.2-54.5% of aromaticity and 0.6-1.2 and 1.3-3.7 of humification index) in AD of chicken manure. The

results from HSQC NMR spectroscopy and 2D-COS-FTIR spectroscopy demonstrated an accelerating effect of the higher temperature on the evolution of HA through humification. Moreover, the concurrent decomposition and re-polymerization of HA during both AD processes, resulting in positive and negative effects on CH_4 production in the fast and slow CH_4 production stages, respectively. The dynamic interaction was due to variations in the electron transferring ability and structure of the formed HA. The results could not only advance our understanding of the mechanisms of HA evolution and its interaction with the performance of AD process, but also support further research toward improving AD performance by regulating HA formation and transformation.

Keywords: Biogas production; humic substances; humification; redox capacity; re-polymerization

1. Introduction

Anaerobic digestion (AD) is a widely implemented biological technology in agriculture that not only offers an appropriate treatment of various agricultural residuals but also provides essential, clean, and affordable renewable energy to society (Maynaud et al., 2017; Somers et al., 2018). In AD processes, organic matter is degraded via a series of microbially mediated reactions initiated by hydrolysis of organic macromolecules into soluble organic units, followed by the production of CH_4 and CO_2 by degrading these soluble compounds via the pathways of acidogenesis, acetogenesis, and methanogenesis (Martins das Neves et al., 2009; Sepehr et al., 2018). The occurrence of these biological degradations leads to the production of a great variety of organic

components such as polyphenols and polysaccharides that can form recalcitrant macromolecular organics, such as humic substances (HS), through the re-polymerization process (Sánchez-Monedero et al., 1999; Baddi et al., 2009). Thus, humic acid (HA), as a major fraction of HS has shown to be a bulk component and usually accounts for 10–20% of the total solids in the anaerobic digesters, with 5–10 g/L of content, which varies depending on the feeding materials and operational conditions (Yap et al., 2018; Guo et al., 2019).

The HA has been deemed a complicated macromolecule that contains many active functional groups, such as carboxylic acid, phenolic, and quinone types (Said-Pullicino et al., 2016; Nie et al., 2018). Recently, the impact of HA on AD performance has increasingly attracted the attention of scientists, and some laboratory experiments have been conducted to study the interaction through the addition of commercial HA or HA analogs in the AD process (Yap et al., 2017; Li et al., 2019a; Bai et al., 2019). The main mechanistic hypothesis concluded from these investigations on the inhibiting impact of HA on the AD performance is due to the binding of active functional groups in HA to the active sites of relevant key enzymes (such as hydrolytic enzymes), thereby preventing their access to substrates (Yap et al., 2017). Moreover, HA has recently been reported to serve as terminal electron acceptors during microbial respiration and function as electron shuttles driving the anaerobic oxidation of methane (Bai et al., 2019) and accelerating the consumption of organic substances during the AD process (Wang et al., 2019). Although a few recent studies have observed the inhibiting effect of commercial HA on the AD process, which is indicated by the reduced CH_4 production, the conclusions may hardly be applied to understand the impact of genuine HA that naturally forms in

69 the AD process (Yap et al., 2017 and 2018; Li et al., 2019b). The structure and function
70 of the commercial HA are relatively consistent during the whole AD experiment, which
71 is insufficient to be representative of the naturally formed HA with dynamic abundance,
72 active functional groups, and electron transferring abilities in different phases of the AD
73 process (Tang et al., 2018; Ma et al., 2019). Therefore, *in-situ* monitoring of naturally
74 formed HA with dynamic characteristics is crucial for re-evaluating and understanding
75 the underlying mechanisms of the effect of HA on AD performance.

76 The process of HA formation, also called humification, involves various microorganism-
77 dominated biological and biochemical processes (Hayes et al., 2009; Mylotte et al.,
78 2016). To date, different hypotheses, including lignin-protein theory, polyphenol theory,
79 and sugar-amine condensation theory, have been used to explain the humification (Tan,
80 2014; Wu et al., 2017; Gao et al., 2019). Generally, the complex organic compounds
81 containing HA precursors could first be decomposed into small-molecule organics and
82 then transformed into recalcitrant macromolecular organic products through the
83 repolymerization to form HA under relevant microorganism functions (Gao et al., 2019).
84 For example, Tang et al. (2020) found the original HA in extracellular polymeric
85 substances could be degraded and modified, and HA with abundant aromatic sites may
86 also bridge protein condensation to regenerate HA during sewage sludge AD process
87 (Tang et al., 2020). Moreover, during humification, precursors from different sources
88 (feeding materials in the AD process) would enable the formation of HA with different
89 molecular compositions, structures, and functionalities due to the different elemental
90 compositions and properties of raw materials (Sale et al., 2015; He et al., 2018). Likewise,
91 the fermentation temperature could also affect the humification pathway and the

92 stability of the formed HA (Jiang et al., 2015; Onwosi et al., 2017). Nevertheless, current
93 knowledge about HA formation mechanisms is largely derived from research on
94 composting, which is primarily led by a group of aerobic microorganisms (Gao et al.,
95 2019; He et al., 2015). Although the phenomenon of HA formation has been observed
96 in the anaerobic digestion (Tang et al., 2018; Tang et al., 2020), the evolutionary
97 dynamics of HA in the AD process, which is dominated by anaerobic microorganisms,
98 have not yet been fully understood (Appels et al., 2008), particularly under conditions
99 with varying feeding materials and operating temperatures. Moreover, information on
100 the dynamics of active functional groups and the electron transferring ability of the
101 naturally formed HA in the entire AD process and its interaction with CH_4 production is
102 insufficient.

103 To address this knowledge gap, we investigated the evolutionary dynamics of genuine
104 HA and its interaction with CH_4 production during different stages of AD processes with
105 two feeding materials, chicken manure and corn stover, under mesophilic (37 °C) and
106 thermophilic (55 °C) conditions. In addition to HA abundance, changes in the structure
107 and active functional groups of HA were determined by two-dimensional correlation
108 (2D-COS) of a Fourier transform infrared spectra (FTIR) and one-bond $^{1}H–^{13}C$
109 heteronuclear single quantum coherence (HSQC) nuclear magnetic resonance (NMR)
110 spectra. The dynamics of the electron transfer capability of HA was detected to elucidate
111 its potential effect on CH_4 generation. Moreover, structural equation modeling (SEM)
112 and principal component analysis (PCA) combined with the results from pyrolysis–gas
113 chromatography/mass spectroscopy (Py-GC/MS) were conducted to reveal the
114 underlying HA evolution mechanisms and their interactions with CH_4 production.

2. Materials and methods

2.1 Setup of the batch AD experiments

Batch AD experiments were conducted in this study using 120 mL serum bottles with a working volume of 60 mL. The commonly used AD feeding materials (chicken manure and corn stover) were fermented under mesophilic (37 °C) and thermophilic (55 °C) conditions for 40 days. The chicken manure was collected from the Deqingyuan biogas plant, which is located in the suburbs of Beijing, China. The total solid (TS) and volatile solid (VS) contents of the chicken manure were 10.01% and 7.88%, respectively (Table 1). The corn stover was obtained from the University farm of China Agricultural University in Beijing, China, and had TS and VS values of 85.90% and 73.12%, respectively (Table 1). Likewise, the sludge from long-term laboratory-scale mesophilic (37 °C) digesters fed with chicken manure (TS of 4.98% and VS of 2.23%) and corn stover (TS of 6.75% and VS of 3.45%) were used as the corresponding inoculum for the AD of chicken manure and corn stover, respectively. Moreover, the sludge from long-term laboratory-scale mesophilic (55 °C) digesters fed with chicken manure (TS of 5.01% and VS of 1.98%) and corn stover (TS of 6.52% and VS of 3.05%) were used as the corresponding inoculum for the AD of chicken manure and corn stover, respectively. The organic matter ratio of the substrate and the inoculum was 1:2 (Guo et al., 2018). The experimental AD bottles were marked and placed in a temperature-controlled incubator (RZH-380A, artificial climate chamber, China), and each treatment was performed in triplicate. Four replicate bottles filled with inoculum alone were used as blanks in each treatment group under the same experimental conditions. Further details on the setup of the batch experiments can be found in Text S1 of the Supporting Information.

Table 1

Characteristic of chicken manure, corn stover and inoculum sludge

Parameters	pH	TS (%)	VS (%)	VS/TS (%)
Chicken manure	7.52±0.20	10.01±0.50	7.88±0.41	78.72±0.32
Corn stover	/	85.90±0.45	73.12±0.38	85.10±0.61
Inoculum sludge (Chicken manure, 37℃)	7.89±0.09	4.98±0.25	2.23±0.17	44.78±0.43
Inoculum sludge (Chicken manure, 55℃)	7.95±0.12	5.01±0.31	1.98±0.26	39.52±0.52
Inoculum sludge (Corn stover, 37℃)	7.22±0.11	6.75±0.18	3.45±0.14	51.11±0.29
Inoculum sludge (Corn stover, 55℃)	7.19±0.13	6.52±0.16	3.05±0.11	46.78±0.12

Daily biogas production was measured using a water displacement manometer (GF-500, KIMO, France). The biogas composition was analysed via gas chromatography with a thermal conductivity detector (SP 2100, BFRL, China). The Gompertz model was used to fit the measured CH_4 yield and identify two CH_4 production stages (fast and slow) (Zhang et al., 2014). The digested slurry was regularly sampled every five days and then immediately analysed in the laboratory for physicochemical properties, including pH, total solids, and volatile solids (VS), according to the standard methods (APHA, 1998; Luo et al., 2018). Further details on the analysis of these physicochemical properties are described in Text S2-1 of the Supporting Information.

2.2 Characteristics of fluorescent components

The excitation–emission matrix (EEM) spectra were recorded using a fluorescence spectrophotometer (Aqualog, HORIBA) to analyze the evolution of the OM in the AD process. The sampled digested slurry was first diluted with distilled water 50 times

153 before the fluorescence spectra analysis. The emission wavelengths (250–550 nm) and
154 excitation wavelengths (250–600 nm) over the range were observed in 5 and 3 nm
155 increments, respectively. The Rayleigh and Raman scattering of the EEM data were
156 calibrated using the method described by Bahram et al. (2006). Finally, parallel factor
157 (PARAFAC) analysis was carried out using MATLAB R2018a (MathWorks, USA) with the
158 DOMFluor Toolbox. Moreover, the fluorescence parameters, including biological index
159 (BIX) and humification index (HIX), were obtained using the data collected through
160 fluorescence spectroscopy. Further detailed information on the EEM and PARAFAC
161 analyses are described in Text S2-2 of the Supporting Information.

162 **2.3 Extraction of humic acid in the sampled digested slurry**

163 The extraction and purification of the HA fraction in the sampled digested slurry were
164 conducted according to the standard method recommended by the International Humic
165 Substances Society (Swift et al., 1996). Briefly, the sampled digested slurry was first
166 shaken (200 rpm, 24 h) with a mixed solution of 0.1 M $Na_4P_2O_7$ and 0.1 M NaOH at a
167 1:10 (w:v) ratio at room temperature. The supernatant was filtered through a 0.45 µm
168 Millipore membrane after 20 min of centrifugation (11,000 rpm). The procedure was
169 repeated three times, and the supernatant was filtered through a 0.45 µm Millipore
170 membrane, acidified with 6 M HCl to pH 1 and left overnight. The precipitate was
171 separated from the liquid phase by centrifugation (5000 rpm, 10 min), suspended in 100
172 ml NaOH and $Na_4P_2O_7$ mixed solution and shaken overnight. The solution was then
173 centrifuged (5000 rpm, 10 min), and the liquid phase was acidified with 0.1 M HCl/0.3
174 M hydrogen fluoride to pH 1, left to stand overnight and centrifuged. The precipitated

was dialyzed against distilled water until Cl^- could no longer be detected (Zhao et al., 2020).

2.4 Humic acid characterization

The carbon (C), hydrogen (H), and nitrogen (N) contents of HA were analysed using an elemental analyzer (Vario EL cube, Germany); the H/C, C/N, and C/O ratios were calculated to analyse the elemental characteristics of HAs. The parameter-specific UV absorbance at 254 nm and 280 nm was measured using a UV-vis spectrophotometer (Shimadzu, UV-2600). SUVA254 is used to characterize the relative aromaticity of HA (Weishaar et al., 2003); similarly, SUVA280 is suitable for tracking the π-π* electron transitions in the UV range (270–280 nm) for phenolic substances, aniline derivatives, benzoic acids, polyenes, and polycyclic aromatic hydrocarbons (Tang et al., 2018). The content changes in the aliphatic and aromatic components of HA were complemented by one-bond $^{1}H–^{13}C$ HSQC NMR spectra using an Avance III 600 MHz spectrometer (Bruker, The Woodlands, TX). Detailed information on this method is described in Text S2-3 (Supporting Information).

FTIR spectra, a mainstream tool for determining functional groups and analyzing the structural composition of sampled HA, was utilized in this study using a Nicolet IS10 FTIR spectrophotometer from 4,000 to 400 cm^{-1} (Zhou et al., 2014). Then, two-dimensional correlation spectra (2D-COS) were used to improve the spectral resolution and characterize the changing degree and order of different functional groups under different conditions. The interpretation of the synchronous and asynchronous plots obtained from 2D-COS was mainly based on Noda's rule (Noda and Ozaki, 2004); additional details are provided in Text S2-4 (Supporting Information).

198 To further investigate the qualitative characterization of the molecular composition of
199 the extracted HA in this study, pyrolysis–gas chromatography/mass spectroscopy (Py-
200 GC/MS) analysis was performed on a Pyroprobe pyrolyzer (6890 GC/5973 MSD, Agilent,
201 USA). Py-GC/MS analysis for each sample was repeated twice and found to have proper
202 repeatability. The compounds obtained through GC/MS were identified via the NIST
203 database by closest match in the NIST MS Search 2.3 using identity-type searching. The
204 threshold for the match factor was 85% (Shahbeig and Nosrati, 2020). The detailed
205 information can be found in Text S2-5 (Supporting Information).

206 To explore the potential of HA to serve as terminal electron acceptors during microbial
207 respiration and function as electron shuttles to drive the redox bioconversion of organic
208 molecules in the AD process (Tan et al., 2017), the electron transfer capacities (ETCs),
209 including the electron-donating capacity (EDC) and electron-accepting capacity (EAC) of
210 HA, were measured using mediated electrochemical reduction and oxidation methods
211 (Wang et al., 2020). Detailed information on this method is described in Text S2-6
212 (Supporting Information).

213 **2.5 Principal component analysis and structural equation modelling**

214 PCA was used to identify different AD performance patterns during the entire AD
215 process at different temperatures. The components used for PCA included CH_4
216 production, HIX, and all the OM components during the AD process of chicken manure
217 and corn stover. A cluster analysis was performed according to the eigenvalues of each
218 component, and the results were used to group similar patterns in the PCA coordinates.
219 SEM was then used to clarify the direct and indirect relationships between HA formation
220 and its impact on the AD process (Gao et al., 2019). Before SEM analysis, auto-regressive

correlation structures were used to identify potential autocorrelations in the IBM SPSS AMOS 23.0 data. Then, we established an *a priori* model according to our current knowledge of HA formation and interaction with CH_4 production, and the data matrix was fitted to the model using the maximum-likelihood estimation method with AMOS 23.0 software (SPSS Inc., Chicago, IL). The χ-square test in SPSS software was used to verify the quality of the fit. Finally, we determined the structural changes of HA and the factors affecting CH_4 production, and we calculated the weight of each factor's influence on CH_4 production.

3. Results and discussion

3.1 Organic matter transformation in the AD process

During the mesophilic AD process, approximately 12% and 2% of the cumulative CH_4 yields of chicken manure and corn stover (254±7 and 227±6 mL gVS^{-1}, respectively) were lower than the yields obtained in the thermophilic AD process (327±9 and 321±10 mL gVS^{-1}, respectively) (Fig. 1a and b). CH_4 generation in AD was mainly achieved by the microbially mediated transformation of the organics (Martins das Neves et al., 2009; Sepehr et al., 2018), and higher temperature fermentation conditions had the advantage of increasing the hydrolysis rate of organics toward increased CH_4 production (Croce et al., 2016). These results were also supported by the higher degradation of VS in the thermophilic AD process (39.6% and 39.6% for chicken manure and corn stover, respectively) than those in the mesophilic AD process (38.3% and 34.8% for chicken manure and corn stover, respectively) (Table S1 and S2). Along with the AD process, the CH_4 production rate is strongly replied on the microbial degradation rate of the organic matter. Based on this concept, the Gompertz model, as a classical kinetic model, has

been developed to simulate the CH_4 production and distinguish different stages of the CH_4 production rates in AD process (Zhang et al., 2014). According to the determined daily CH_4 generation (Fig. S1) and the theoretical Gompertz model, the transmission of fast (stage I, Fig. 1) and slow (stage II, Fig. 1) CH_4 production stages were identified for the AD of chicken manure (day 10) and corn stover (day 18) without differences between the mesophilic and thermophilic conditions.

PARAFAC analyses based on the EEM fluorescence spectra were used to illustrate the transformations of OM in the AD process (Fig. 2a–h). Five fluorescent components were identified (Table S3), comprising two humic-like compounds (C1 and C3), one fulvic-like compound (C2), protein-like and tyrosine-like substances (C4), and tryptophan-like substances (C5) (He et al., 2015; Wang et al., 2020). Among them, the abundance of protein-like components decreased with an increase in the humic-like components during the AD process for both materials (Fig. S2). Along with the transformation of OM, the content of HA decreased from 8.4 ± 0.9 to 4.6 ± 0.6 g L^{-1} in the fast CH_4 production stage and then gradually increased to 7.7 ± 0.8 g L^{-1} during the slow CH_4 production stage of the mesophilic AD of chicken manure (Fig. 1c). However, under the thermophilic conditions, the content of HA continuously decreased from the initial value of 6.8 ± 0.7 to 4.1 ± 0.4 g L^{-1} in the fast CH_4 production stage and maintained a similar level until the end of the experiment. The dynamics of the HA content in the AD of corn stover showed a different tendency (Fig. 1d). The HA content increased from 4.5–4.9 to 7.1–7.5 g L^{-1} in the first five days and then decreased to 3.9–4.1. g L^{-1} in the fast CH_4 production stage under both temperature conditions. In the slow CH_4 production stage, the HA content gradually increased to 4.6–5.2. g L^{-1} by day 40.

Integrating the dynamics of HA content during the AD process (Fig. 1c and d) indicated the concurrent decomposition and formation of HA during the AD process. It was reported that the initial HA content in the feeding material and/or inoculum would first degrade in the fast CH_4 production stage along with the biodegradation of the organics (Tang et al., 2018); however, in the following slow CH_4 generation stage, essential precursors to the formation of HA, such as polyphenols, carboxylic acids, and amino acids via the transformation of the OM, could be generated and lead the re-polymerization of HA (Gao et al., 2019). Notably, the fast HA content increase in the early stage for corn stover (Fig. 1d) may be attributed to the abundance of fiber-structural components (e.g., lignin), which provides more stable phenolic compounds required as starting materials for humification processes (Lopez et al., 2002). Moreover, significantly lower HA contents were quantified under the thermophilic conditions than in the mesophilic conditions, indicating the stimulating effect of higher temperatures on HA degradation (Putranto et al., 2017). This can be attributed to the faster microbial degradation of polysaccharides, proteins, and fats to CH_4 instead of re-polymerization to HA (Jiang et al., 2015; Onwosi et al., 2017), which results in higher biogas production under the thermophilic AD process (Fig. 1a and b).

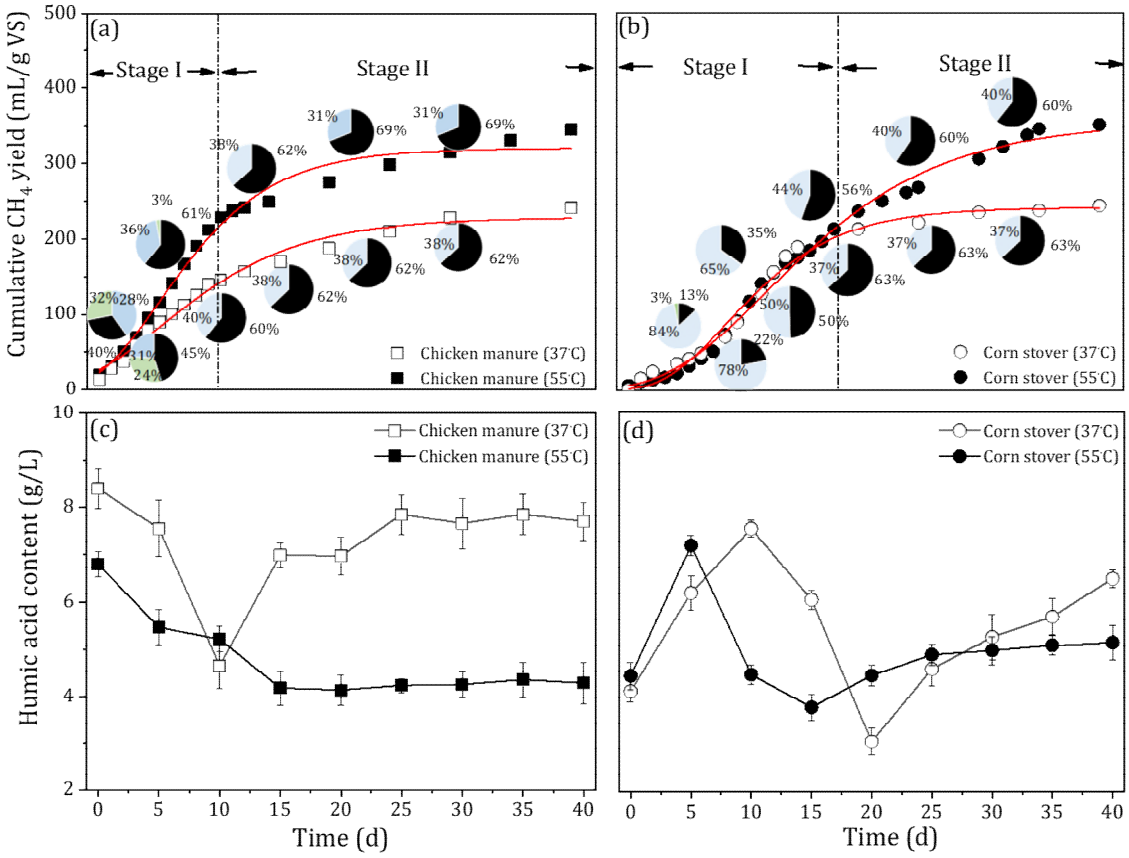

Fig. 1. The cumulative methane produced and humic acid content during chicken manure (a, c) and corn stover (b, d) anaerobic digestion at different temperatures. The black, blue, and green areas in the pie chart represent methane, carbon dioxide, and nitrogen content, respectively (Stage I: fast methane production stage; Stage II: Slow methane production stage).

3.2 Characterization of the humification process

Target fluorescence indexes, including biological index (BIX) and humification index (HIX), were calculated to evaluate the characteristics of the humification process for HA formation in different AD processes (Fig. 2i–l). BIX is commonly used to evaluate the autochthonous biological activity of the formed HA, where a high BIX value corresponds to the presence of freshly produced HA (Tedetti et al., 2011; He et al., 2015). In this study, the declining trend of the BIX value in both AD processes of chicken manure (from 1.01–1.06 to 0.65–0.69) and corn stover (from 0.95–1.03 to 0.81–0.82) represented the aging process of the freshly formed HA to the humified structure. Besides, HIX is a general

298 indicator of the degree of humification of HA and is positively related to the complexity
299 of the structure (Huguest et al., 2009). The HIX values of the formed HA in the
300 thermophilic AD process (1.26–3.68) were significantly higher than those in the
301 mesophilic AD of chicken manure (0.58–1.18), indicating the positive effect of higher
302 temperature on the HA humification process (Fig. 1c) (Guo et al., 2019).

303 Although the temperature effect on HIX in the AD of corn stover was not significant, the
304 continually increased values (from 1.49–2.77 to 4.19–4.52) indicated the strengthened
305 humification process during the AD process under both temperature conditions (Fig. 2k
306 and l). The influence of temperature on HIX formation is different for distinct substrates
307 may due to the composition of the corn stover has abundant lignocellulosic compounds
308 compared with chicken manure (Gao et al., 2019). To confirm these changes in the
309 structure of HA, the levels of the aromaticity of HA in different AD processes were
310 further determined by HSQC NMR spectroscopy (Fig. S3). Similarly, the results showed
311 a higher increase in the aromaticity (30.2–68.4%) in the HA formed in the thermophilic
312 AD process than those (28.3–66.7%) in the mesophilic AD process (Table S4), which
313 agreed with the changes in BIX and HIX. The degradation of superficial labile aliphatics
314 in HA was improved under thermophilic conditions, which might be the reason for the
315 increase in the degree of humification during the thermophilic AD process (Tang et al.,
316 2018).

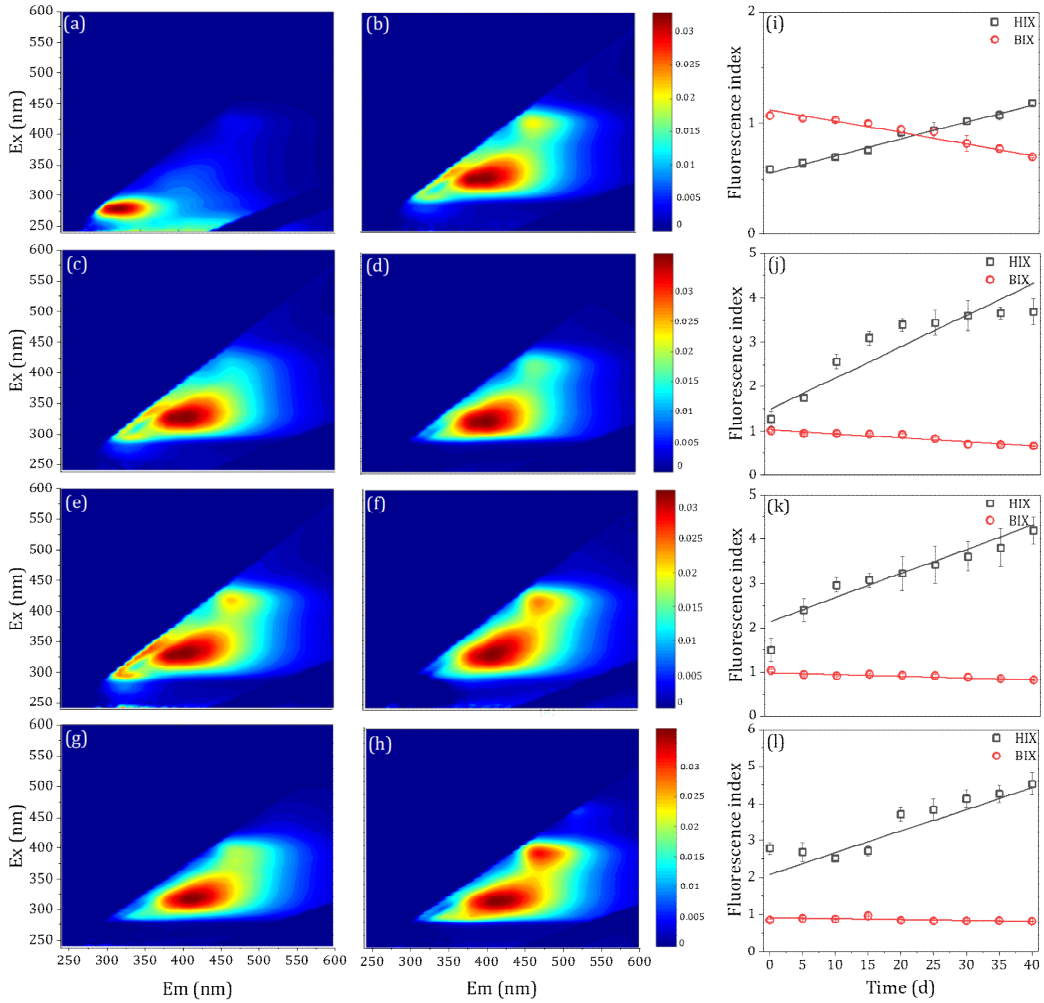

317

318 **Fig. 2.** Excitation–emission matrix fluorescence spectra of OM, and the humification index (HIX)
319 and biological index (BIX) evolution during the mesophilic and thermophilic anaerobic digestion of
320 chicken manure and corn stover. (a, b) mesophilic anaerobic digestion of chicken manure at 0 and
321 40 days; (c, d) thermophilic anaerobic digestion of chicken manure at 0 and 40 days; (e, f) mesophilic
322 anaerobic digestion of corn stover at 0 and 40 days; (g, h) thermophilic anaerobic digestion of corn
323 stover at 0 and 40 days; (i, j) HIX and BIX from the mesophilic and thermophilic anaerobic digestion
324 of chicken manure, respectively; (k, l) HIX and BIX from the mesophilic and thermophilic anaerobic
325 digestion of corn stover, respectively.

326 **3.3 Variation in the functional groups of HA**

327 Due to the complex structure of HA, the simple FTIR image (Fig. S4) cannot identify the
328 changes in the functional groups based on the obtained infrared absorption spectra
329 (Gao et al., 2019). Thus, a further 2D-COS analysis was applied to examine the structural
330 changes in the active functional groups of HA (Fig. 3). In the synchronous 2D-COS IR

spectra, a total of six auto-peaks (at 3000, 3400, 1850, 1700, 1230, and 1030 cm^{-1}) and six positive cross-peaks at (1030, 3000), (1700, 3000), (1030, 1850), (1230, 1700), (1700, 1850), and (1850, 3000) were determined, and no significant difference between the mesophilic and thermophilic AD of chicken manure and corn stover was observed (Fig. 3a–d). Notably, the intensity of the auto-peaks in the 2D-COS IR spectra for HA formed from the mesophilic AD process was lower than that from the thermophilic AD process.

Compared with the synchronous maps, the asynchronous 2D-COS analyses of HA formed from the chicken manure and corn stover AD processes showed significant differences, with only cross-peaks detected (Fig. 3e–h). The asynchronous map of HA produced during the AD (mesophilic and thermophilic) of chicken manure contained seven negative cross-peaks at (1030, 3400), (1600, 3400), (2800, 3400), (1230, 3400), (1030, 1700), (1230, 1700), and (1850, 3400), and two positive cross-peaks at (1600, 1700) and (1600, 2800). Unlike the chicken manure, three positive cross-peaks at (1600, 3000), (1600, 1700), and (2800, 3000) and five negative cross-peaks at (1850, 3000), (1230, 3000), (1030, 1600), (1230, 1600), and (3000, 3400) were observed for HA formed during the (mesophilic and thermophilic) AD of corn stover. According to Noda's rules (Noda and Ozaki, 2004), the peaks reacted in the following order: 2800 cm^{-1} > 3400 cm^{-1} > 1700 cm^{-1} > 1030 cm^{-1}, 1230 cm^{-1} > 1600 cm^{-1}, 1850 cm^{-1} for the AD of chicken manure, and 3400 cm^{-1} > 2800 cm^{-1} > 1850 cm^{-1}, 1600 cm^{-1} > 1700 cm^{-1} > 1230 cm^{-1}, 1030 cm^{-1} for the AD of corn stover. Therefore, the active functional groups of HA formed in the chicken manure AD process changed in the sequence of aliphatic-like substances (C-H) > amides (H-N) or carbohydrates (O-H) > carboxylic acids (C=O) > polysaccharides (C=O), phenol > aromatic compounds, ketones (C=C). The active functional groups of HA

formed in the corn stover AD process changed in the following sequence: amides (H-N) or carbohydrates (O-H) > aliphatic-like substances (C-H) > aromatic compounds and ketones (C=C) > carboxylic acids (C=O) > polysaccharides (C=O), phenolics (Gao et al., 2019; Yang et al., 2019).

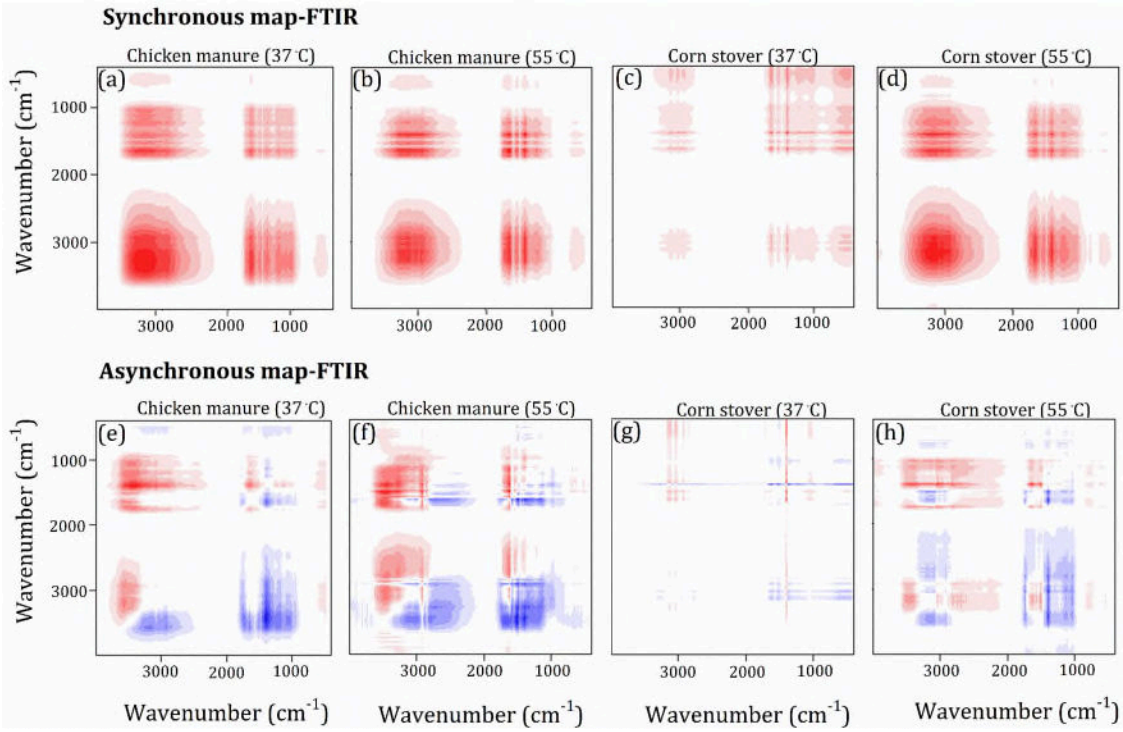

Fig. 3. 2D-FTIR correlation maps generated from the 400–4000 cm^{-1} region of the spectra of humic acid in the anaerobic digestion of chicken manure and corn stover at different temperatures. Red and blue represent positive and negative correlations, respectively. A more intense color indicates a stronger correlation.

3.4 Redox capability evolution of HA

The redox capabilities of the HA transformed during the AD of chicken manure and corn stover were assessed by the ETCs of HA (Fig. S5), including the EAC and EDC. The ETCs (both EAC and EDC) of HA increased during the mesophilic and thermophilic AD of chicken manure and corn stover, which indicated the increased capability of the formed HA to influence the microbially mediated organics transformation process (Tan et al., 2017; Zhao et al., 2020). Moreover, both feeding materials and fermentation

370 temperatures significantly affect the redox capability evolution of HA. The ETC values of
371 HA during the mesophilic AD of chicken manure (671 ± 15–1469 ± 23 μmol gHA^{-1}) and
372 corn stover (687 ± 20–1294 ± 25 μmol gHA^{-1}) were lower than those (774 ± 22–1515 ±
373 18 μmol gHA^{-1} and 1013 ± 19–1424 ± 21 μmol gHA^{-1} for chicken manure and corn stover,
374 respectively) in the thermophilic AD processes. The results indicated that higher
375 temperatures could facilitate an increase in the ETCs of HA (Tan et al., 2017).

376 The ETCs of HA could contribute to the microbially mediated reactions in the AD process
377 and influence organic transformation and CH_4 generation (Bai et al., 2019). Such redox
378 capacity heavily depends on the structure/composition of HA, such as basic elements (C,
379 N, H, and O) and their ratios (C/H, C/N, and C/O), relative aromaticity ($SUVA_{254}$), π-π*
380 electron transitions ($SUVA_{280}$), functional groups from FTIR detections, and humification
381 degree (HIX and BIX). Thus, Pearson correlation analysis was conducted to evaluate the
382 influence of the characteristics (Table S5, S6, and S7) on the redox capacity of HA for
383 both feeding materials under different temperature conditions (Fig. 4). During the AD of
384 chicken manure, the ETC (EAC and EDC) was positively related to the HIX, element N,
385 $SUVA_{254}$, $SUVA_{280}$, carbonyl group, carboxyl group, and ketone group and was negatively
386 correlated with the BIX and C/N ratio. Compared with the chicken manure AD process,
387 only the HIX, carbonyl group, and carboxyl group were positively correlated with the ETC
388 of HA during corn stover AD processes. The obvious effect of the two feeding materials
389 was addressed, which may be due to the distinct organic sources for the AD process (He
390 et al., 2014).

391

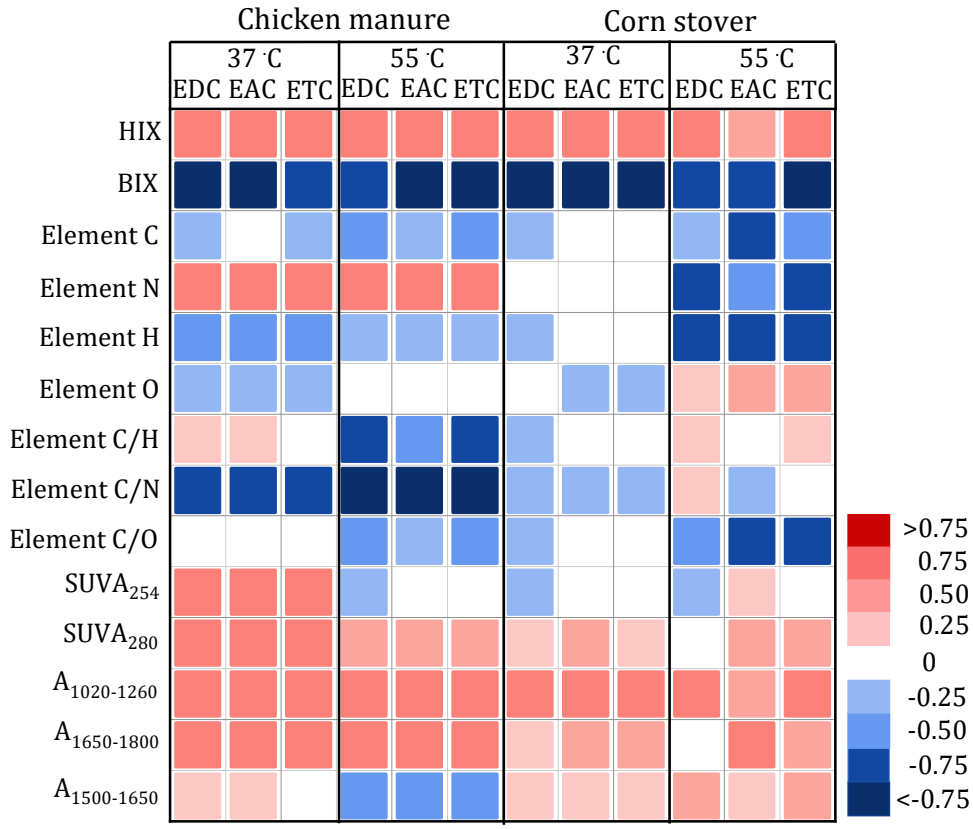

Fig. 4. Correlation between the chemical structure and redox properties of humic acid derived from chicken manure and corn stover anaerobic digestion. (EDC: Electron-donating capacity; EAC: Electron-accepting capacity; ETC: Electron transfer capacity; HIX: Humification index; BIX: Biological index; $A_{1020–1260}$: The area of 1020–1260 cm^{-1} from FTIR represents the oxygen-containing groups (such as the carbonyl group and carboxyl group); $A_{1650–1800}$: The area of 1650–1800 cm^{-1} from FTIR represents the ketone groups; $A_{1500–1650}$: The area of 1500–1650 cm^{-1} from FTIR represents the N-H and amide groups)

3.5 Mechanisms of HA evolution and interaction with CH_4 production

PCA and SEM were performed to explore the potential HA evolution pathways in the AD process with different feeding materials and temperatures (Fig. 5). Three obvious groups were identified in the PCA coordinates for both the AD of chicken manure (Fig. 5a) and corn stover (Fig. 5b). For both materials, the samples from the fast CH_4 production stage were grouped without identifiable differences from the temperature conditions. The group was located in the up-left area of the coordinate, which was positively contributed by the PCA component of CH_4 production and negatively contributed by the HIX. It

indicates that the humification (HA formation) in the fast CH_4 production stage does not affect CH_4 production. During the slow CH_4 production stage, the samples from the mesophilic and thermophilic AD processes were separated for both materials. Both groups moved towards the down-right area in the coordinates, which were positively contributed by the PCA component of HIX and negatively contribute by the CH_4 production. The results represent the significant inhibitory effect of HA on CH_4 generation at this stage of the AD process. Moreover, the higher factor contribution of the HIX was observed in the thermophilic AD group, which supported the negative influence of HA on CH_4 production being stronger under thermophilic conditions than under mesophilic conditions. When looking at the HA structures, the results from PCA showed that the protein-like substances (C4 and C5) were negatively correlated with humic-like substances (C1 and C3) and HIX, indicating the potential contribution of the degradation of protein-like substances to HA humification (Hardie et al., 2009; Zhang et al., 2015).

SEM is an effective method to study the complex relationships between latent and observed variables (Liu et al., 2019), and it has been widely used to interpret and predict interactions in multivariate datasets (Grace, 2006; Gao et al., 2019). In this study, SEM was used to elucidate the HA evolution along with the organic transformation and CH_4 production. The results showed a complex interaction among aliphatic compounds, aromatic compounds, amides, carboxyl acids, and HA structural characteristics (Fig. 5c–f). Generally, in the AD process of chicken manure, amides and aliphatic compounds negatively affect HA structural characteristics but positively influence small molecules, such as carboxyl acids; however, in the AD process of corn stover, carbohydrates and

aliphatic compounds have a significantly positive effect on amides, which indirectly influence the HA structural characteristics (Fig. 5d). The contents of amide and aliphatic components in HA have a significantly positive influence on CH_4 production during the fast CH_4 production stage of the chicken manure and corn stover AD processes (Fig. 5c and d). The higher aromatic components in HA have significantly negative impacts on CH_4 production during the later slow CH_4 production stage (Fig. 5e and f). The results indicated that the impact of HA on AD performance significantly depends on the humification degree or aromaticity of HA (Yap et al., 2017; Li et al., 2019a). The aliphatic compounds, amides, and carbohydrates in less humified HA can first be degraded to serve as the carbon resource for microorganisms to produce CH_4 (Tang et al., 2018). When the HA structure becomes more complex and stable with higher aromaticity, an inhibitory effect on CH_4 production may appear (Li et al., 2019b).

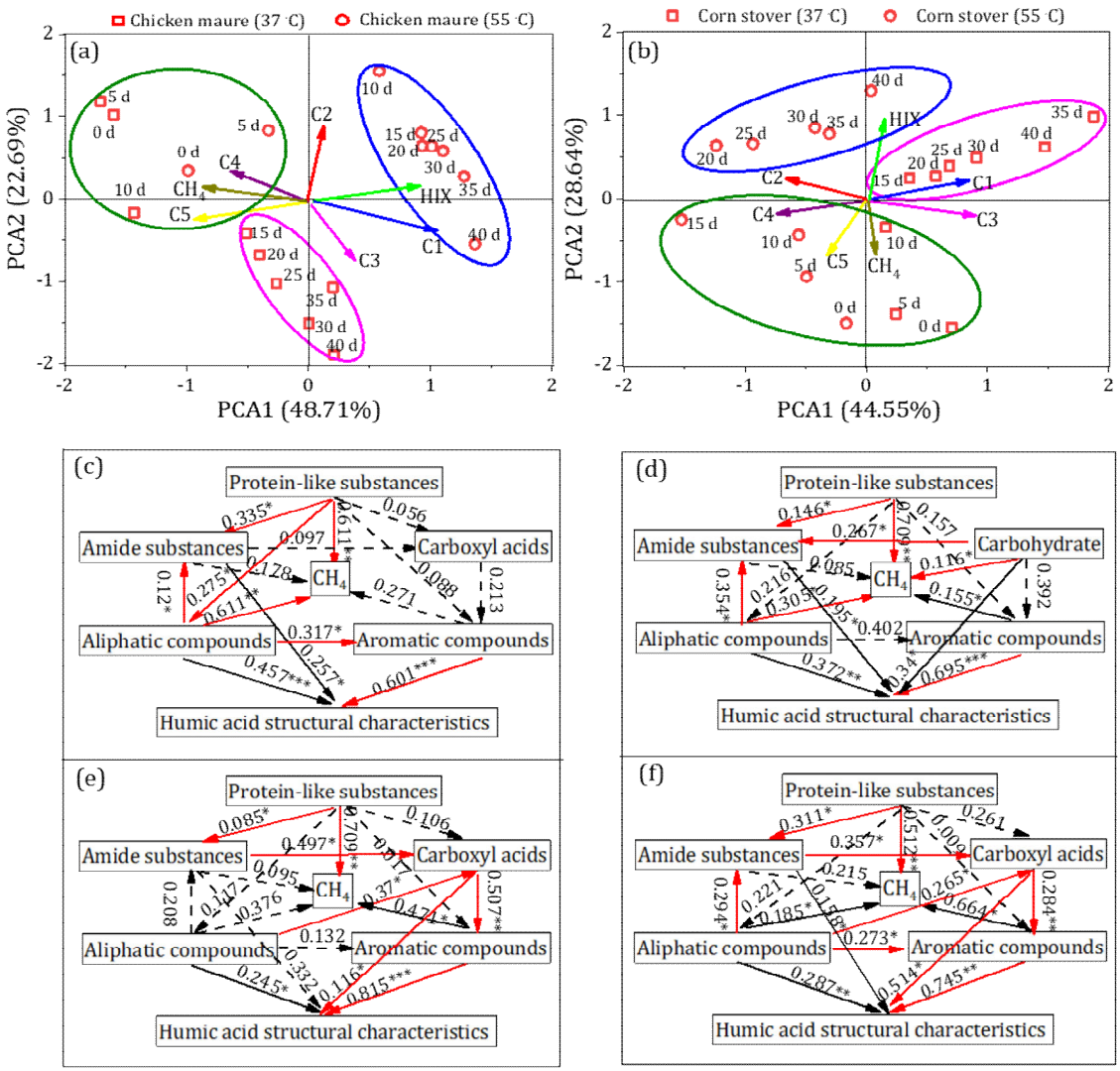

Fig. 5. Principal component analysis biplot considering the changes in organic matter during the anaerobic digestion process with (a) chicken manure and (b) corn stover at different temperatures. A structural equation model (SEM) showing the direct and indirect effects of the key factors on HA formation and methane production in the fast methane production stage and slow methane production stage of chicken manure (c), (e) and corn stover (d), (f) anaerobic digestion. The path coefficients are adjacent to the arrows, *p < 0.05; **p < 0.01; ***p < 0.001. (HIX: humification index; C1, C3: humic acid-like substance; C2: Fulvic acid-like substance; C4: Tyrosine-like substance; C5: Tryptophan-like substance)

To evaluate the possible transformation and decomposition pathways of HA during the AD process, the species and quantities of HA compositions were assessed in both the fast and slow CH_4 production stages using Py-GC/MS (Fig. S6). The main compositions of the HA from the AD of chicken manure and corn stover were slightly different; however,

457 they can be generally categorized into aldehydes, alcohols, amines, acids, ketones,
458 benzenes, phenols, and hydrocarbons (Table S8 and S9). Based on the aforementioned
459 information, the potential mechanism of HA transformation during the AD process is
460 summarized in Fig. 6. In the chicken manure AD process (Fig. 6a), the initial basic
461 structural units of HA, which are composed of a variety of easily degradable substances
462 (such as aliphatic compounds, amides, and protein), were first degraded to contribute
463 to CH_4 production in the fast CH_4 production stage (Tang et al., 2018; Gao et al., 2019).
464 Then, the small molecules, such as those with carboxyl-rich groups of aromatic
465 compounds and amide compounds, attached to these basic units of HA by condensation
466 reactions and finally formed more complex and humified structures (Sánchez-Monedero
467 et al., 1999; Baddi et al., 2009; Said-Pullicino et al., 2016). However, the formation of HA
468 in the corn stover AD process showed different pathways (Fig. 6b). First, the
469 intermediates from carbohydrate and polyphenol compound degradation are rich in
470 carboxyl and hydroxyl moieties and serve as the precursor of HA to form low-molecular-
471 weight compounds with HA characteristics, such as amides. These compounds react
472 with aromatic-like substances to form a tight polymer that is also regarded as the “core”
473 of HA. Then, in a process similar to the chicken manure AD process, easily degradable
474 compounds (such as aliphatic and polysaccharides) were decomposed. As the
475 fermentation continues, some small-molecule organic acids (e.g., carboxyl), as the
476 intermediates between amide and aliphatic compound degradation, attach to the
477 surface of the core of HA, forming more mature and stable HA macromolecules (Jiang
478 et al., 2015; Wu et al., 2017; Gao et al., 2019).

CH_4 production was also significantly affected by the dynamic electron transferring ability of the formed HA, along with their structural evolution during the AD process (Fig. S7). In the fast CH_4 production stage, the positive effect of HA on CH_4 production may not only be sacrificing aliphatic compounds, amides, and carbohydrates in HA as carbon resources, but may also be facilitating the electron transfer chain among various microbially mediated reactions, such as acidogenesis, acetogenesis, and methanogenesis (Fernandes et al., 2015; Li et al., 2019a). In the following slow CH_4 production stage, however, the functional groups in more humified HA can bind to the active sites of relevant key enzymes in AD (such as hydrolytic enzymes), thereby preventing their access to substrates and resulting in lower CH_4 generation (Yap et al., 2017). The result also provides evidence that the highly humified HA with high ETC has the potential to serve as terminal electron acceptors during microbial respiration and to function as electron shuttles driving the anaerobic oxidation of methane (AOM, Bai et al., 2019). Note that the microbial community and abundance that perform the HA-dependent AOM process were not involved in this study; therefore, the direct relationship between the HA formed by the AD process and the AOM process, functional microbes, and electron transfer mechanisms needs to be further analyzed.

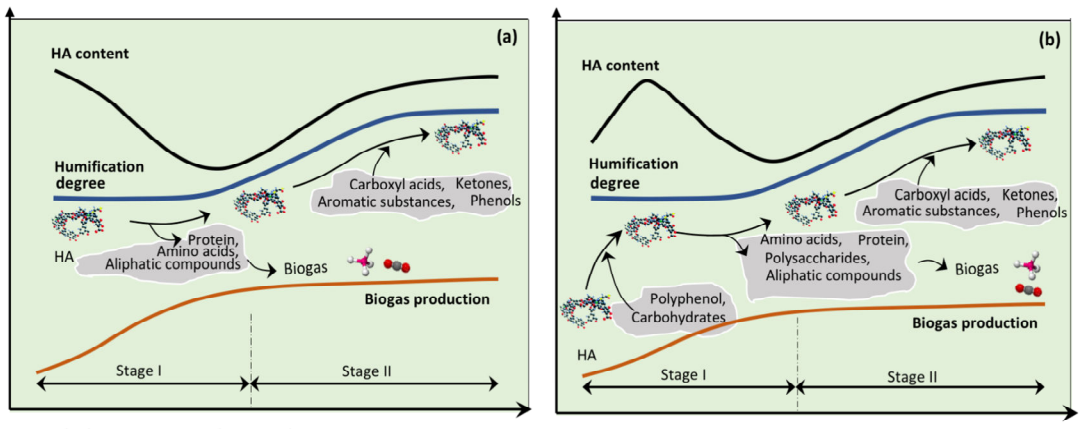

Chicken Manure Batch Anaerobic Digestion Process

Corn Stover Batch Anaerobic Digestion Process

Fig. 6. The possible transformation and decomposition pathways of humic acid during anaerobic digestion with (a) chicken manure and (b) corn stover.

3.6 Significance of this work

The existence of HA formed in the AD system could create a negative effect on the energy efficiency of the conversion of waste OM to CH_4 (Bai et al., 2019; Li et al., 2019b); however, this conclusion was based on previous studies with the external addition of commercial HA, which can hardly reflect the impact of genuine HA that naturally formed in the AD process with a dynamic structure and function. Our research conducted *in-situ* monitoring of the dynamics of HA evolution, including degradation, formation, structure variation, functional groups, and ETC alternation to re-evaluate the interaction effect. The present study proved that the decomposition of aliphatic, amide, carbohydrate, and protein-like compounds in HA positively correlated with CH_4 production in the fast CH_4 production stage, and the accumulation of the re-polymerized HA in the later stage negatively correlated with CH_4 production in the AD process. Moreover, the impact of HA on AD performance is significantly dependent on the humification degree or aromaticity of HA, which varies with fermentation time and temperature. The thermophilic conditions significantly promoted the evolution of the HA structure during the AD process. The formation mechanisms of HA were also different in the AD of different feeding materials, i.e., chicken manure and corn stover. Further studies could investigate the microbial community characterisation in relation to the HA transformation. Nevertheless, with the current results, this study improves our understanding of the transformation of HA itself and its dynamic effects on other carbon metabolism pathways and thus improves the transparency of the knowledge “black box” that exists in the AD process.

From the perspective of engineering applications, this study may provide an evidence-based recommendation for optimising the operations of AD process in order to improve the CH_4 production efficiency. The current applied AD plants are normally operated under a hydraulic retention time of 20-30 days for manures (Li et al., 2020) and 40-50 days for lignocellulosic biomass (Guo et al., 2018; Xu et al., 2020), respectively. Considering the potential interactive effect of genuine HA formed in the AD process on CH_4 production, the current findings may suggest a shorter retention time. However, to consolidate this conclusion, further research is still needed..

4. Conclusions

This study investigated the evolutionary dynamics of the structure and function of genuine HA that naturally formed in the AD processes and re-evaluated its dynamic interaction with CH_4 production. The concurrent decomposition and re-polymerization of HA during the AD process was observed, however, the HA evolution mechanisms in the AD of chicken manure and corn stover showed different pathways. An accelerating effect of the higher temperature on the evolution of HA through humification was also confirmed from the results of HSQC NMR spectroscopy and 2D-COS-FTIR spectroscopy detections. The HA performed positive and negative effects on CH_4 production in the fast and slow CH_4 production stages, respectively. The dynamic interaction was due to variations in the electron transferring ability and structure of the formed HA. The results could support further research and deployment of AD toward improving AD performance by regulating the evolution of the HA.

Acknowledgments

This work was financed by the AIAS-COFUND fellowship Programme, which is funded by the European Union's Seventh Framework Programme for Research, Technological Development and Demonstration under grant agreement no. 609033.

Appendix A. Supplementary data

Supplementary data associated with this article can be found in the Supporting Information. Text S1–S2, additional analytical methods; Figures S1–S7, daily methane production, the relative proportion of fluorescence components, 2D-COS HSQC NMR spectra, FTIR spectra, ETC, Py-GC/MS spectra, and the relationship between ETC and daily methane production; Table S1–S9, characteristics of physicochemical properties of the AD process, EEM spectra PARAFAC analysis, the percent aliphaticity and aromaticity of HA, elemental composition, SUVA values, and typical products by Py-GC/MS analysis.

References

Appels, L., Baeyens, J., Degreve, J., Dewil, R., 2008. Principles and potential of the anaerobic digestion of waste-activated sludge. Prog. Energ. Combus. 34, 755-781.

APHA (American, Public Health Association), AWWA (American Water Works and Protection Association) and WPCF (Water Pollution Control Federation), 1998. Standard Methods for the Examination of Water and Wastewater 20td ed., Washington, D.C.

Bahram, M., Bro, R., Stedmon, C., Afkhami, A., 2006. Handing of Rayleigh and Raman scatter for PARAFAC modeling of fluorescence data using interpolation. J. Chemom. 20, 99-105.

Bai, Y. N., Wang, X. N., Wu, J., Lu, Y. Z., Fu, L., Zhang, F., Lau, T. C., Zeng, R. J., 2019. Humic substances as electron acceptors for anaerobic oxidation of methane driven by ANME-2d. Water Res. 164, 114935.

Baddi, G.A., Cegarra, J., Merlina, G., Revel, J.C., Hafidi, M., 2009. Qualitative and quantitative evolution of polyphenolic compounds during composting of an olive-mill waste-wheat straw mixture. J. Hazard. Mater. 165, 1119–1123.

Croce, S., Qiao, W., D'lmporzano, G., Dong, R., Adani, F., 2016. Anaerobic digestion of straw and corn stover: The effect of biological process optimization and pre-

treatment on total bio-methane yield and energy performance. Biotech. Advan. 34, 1280-1304.

Fernandes, T. V., van Lier, J. B., Zeeman, G., 2015. Humic acid-like and fulvic acid-like inhibition on the hydrolysis of cellulose and tributyrin. BioEnergy Res. 8 (2), 821–831.

Grace, J. B., 2006. Structural Equation Modeling and Natural Systems; Cambridge University Press.

Gao, X., Tan, W., Zhao, Y., Wu, J., Sun, Q., Qi, H., Xie, X., Wei, Z., 2019. Diversity in the mechanisms of humin formation during composting with different materials. Environ. Sci. Technol. 53, 3653-3662.

Guo, X. X., Liu, H. T., Wu, S. B., 2019. Humic substances developed during organic waste composting: Formation mechanisms, structural properties, and agronomic functions. Sci. Total Environ. 662, 501-510.

Guo, J., Cui, X., Sun, H., Zhao, Q., Wen, X., Pang, C., Dong, R., 2018. Effect of glucose and cellulase addition on wet-storage of excessively wilted maize stover and biogas production, Bioresour. Technol. 259, 198-206.

He, X. S., Xi, B. D., Gao, R. T., Wang, L., Ma, Y., Cui, D. Y., Tan, W. B., 2015. Using fluorescence spectroscopy coupled with chemometric analysis to investigate the origin, composition, and dynamics of dissolved organic matter in leachate-polluted groundwater. Environ. Sci. Pollut. Res. 22, 8499-8506.

Hayes, M. H. B., 2009. Evolution of concepts of environmental natural nonliving organic matter; Wiley interscience: New York, NY.

He, S., Ding, L. L., Li, K., Hu, D. H., Ye, L., Ren, H. Q., 2018. Comparative study of activated sludge with different individual nitrogen compositions, metagenomic and microbial community. Bioresour. Technol. 247, 915-923.

Huguest, A., Vacher, L., Relexans, S., Saubusse, S., Froidefond, J. M., Parlanti, E., 2009. Properties of fluorescent dissolved organic matter in the Gironde Estuary. Org. Geochem. 40(6), 706-719.

He, X. S., Xi, B. D., Cui, D. Y., Liu, Y., Tan, W. B., Pan, H. W., Li, D., 2014. Influence of chemical and structural evolution of dissolved organic matter on electron transfer capacity during composting. J. Hazad. Mat. 268, 256-263.

Hardie, A. G., Dynes, J. J., Kozak, L. M., Huang, P. M., 2009. The role of glucose in abiotic humification pathways as catalyzed by birnessite. J. Mol. Catal. A Chem. 308, 114–126.

Lopez, M. J., Elorrieta, M. A., Vargas-Garcia, M. C., Suarez-Estrella, F., Moreno, J., 2002. The effect of aeration on the biotransformation of lignocellulosic wastes by white-rot fungi. Bioresour. Technol. 81, 123–129.

Li, B., Dinkler, K., Zhao, N., Sobhi, M., Merkle, W., Liu, S., Dong, R., Oechsner, H., Guo, J., 2020. Influence of anaerobic digestion on the labile phosphorus in pig, chicken, and dairy manure. Sci. Total Environ. 737, 140234.

Li, J., Hao, X., van Loosdrecht, M. C. M., Luo, Y., Cao, D., 2019a. Effect of humic acids on batch anaerobic digestion of excess sludge. Water Res. 155, 431-443.

Li, J., Hao, X., Loosdrecht, M. C. M., Yu, J., Liu, R., 2019b. Adaptation of semi-continuous anaerobic sludge digestion to humic acids. Water Res. 161, 329-334.

Luo, H., Lyu, T., Muhmood, A., Xue, Y., Wu, H., Meers, E., Dong, R., Wu, S., 2018. Effect of flocculation pre-treatment on membrane nutrient recovery of digested chicken slurry: Mitigating suspended solids and retaining nutrients. Chem. Eng. J. 352, 855-862.

Liu, Y. R., Yang, Z., Zhou, X., Qu, X., Li, Z., Zhong, H., 2019. Overlooked Role of Putative Non-Hg Methylators in Predicting Methylmercury Production in Paddy Soils. Environ. Sci. Technol. 53, 1230-12338.

Jiang, J., Liu, X., Huang, Y., Huang, H., 2015. Inoculation with nitrogen turnover bacterial agent appropriately increasing nitrogen and promoting maturity in pig manure composting. Waste Manag. 39, 78–85.

Ma, S., Hu, H., Wang, J., Liao, K., Ma, H., Ren, H., 2019. The characterization of dissolved organic matter in alkaline fermentation of sewage sludge with different pH for volatile fatty acids production. Water Res. 164, 114924.

Maynaud, G., Druilhe, G., Daumoin, M., Jimenez, J., Patureau, D., Torrijos, M., Pourcher, A. M., Wery, N., 2017. Characterization of the biodegradability of post-treated digestates via the chemical accessibility and complexity of organic matter. Bioresour. Technol. 231, 65-74.

Martins des Neves, L. C., Concert, A., Vessoni Penna, T. C., 2009. Biogas production: new trends for alternative energy sources in rural and urban zones. Chem. Eng. Technol. 32, 1147-1153.

Mylotte, R., Sutrisno, A., Farooq, H., Masoom, H., Soong, R., Hayes, M. H. B., Simpson, A. J., 2016. Insight into the composition of recalcitrant organic matter from estuarine sediments using NMR spectroscopy. Org. Geochem. 98, 155-165.

Noda, I., Ozaki, Y., 2004. Two-dimensional correlation spectroscopy applications in vibrational and optical spectroscopy. John Wiley, England.

Nie, X., Li, Z., Huang, J., Liu, L., Xiao, H., Liu, C., Zeng, G., 2018. Thermal stability of organic carbon in soil aggregates as affected by soil erosion and deposition. Soil Tillage Res. 175, 82-90.

Onwosi, C. O., Igbokwe, V. C., Odimba, J. N., Eke, I. E., Nwankwoala, M. O., Iroh, I. N., Ezeogu, L. I., 2017. Composting technology in waste stabilization: on the methods, challenges and future prospects. J. Environ. Manag. 190, 140–157.

Putranto, A., Chen, X. D., 2017. A new model to predict diffusive self-heating during composting incorporating the reaction engineering approach (REA) framework. Bioresour. Technol. 232, 211–221.

Swift, R. S., Sparks, D. L., Madison, W., 1996. Isolation of IHSS soil fulvic and humic acid from http://humic-substances.org/isolation-of-ihss-soil-fulvic-and-humic-acids/. Exerpt from-organic matter characterization (chap 35). In: Method of soil analysis, pp. 1018-1020. Part 3. Chemical methods. Soil Sci. Soc. Am. Book Series: 5. Soil Sci. Soc. Am.

Said-Pullicino, D., Miniotti, E. F., Sodano, M., Bertora, C., Lerda, C., Chiaradia, E. A., Romani, M., Cesari de Maria, S., Sacco, D., Celi, L., 2016. Linking dissolved organic carbon cycling to organic carbon fluxes in rice paddies under different water management practices. Plant Soil 401, 273-290.

Somers, M. H., Azman, S., Sigurnjak, I., Ghyselbrecht, K., Meers, E., Meesschaert, B., Appels, L., 2018. Effect of digestate disintegration on anaerobic digestion of organic waste. Bioresour. Technol. 268, 568-576.

Sepehr, S. Y., Hedenstrom, M., Stehr, J. E., Dario, M., Hertkorn, N., Bjorn, A., 2018. Pretreatment of anaerobic digester samples by hydrochloric acid for solution-state 1H and 13C NMR spectroscopic characterization of organic matter. Chemosphere, 199, 201-209.

Sánchez-Monedero, M. A., Roig, A., Cegarra, J., Bernal, M. P., 1999. Relationships between water-soluble carbohydrate and phenol fractions and the humification indices of different organic wastes during composting. Bioresour. Technol. 70, 193–201.

Sale, V., Aguilera, P., Laczko, E., Mader, P., Berner, A., Zihlmann, U., van der Heijden, M. G. A., Oehl, F., 2015. Impact of conservation tillage and organic farming on the diversity of arbuscular mycorrhizal fungi. Soil Biol. Biochem. 84, 38-52.

Shahbeig, H., Nosrati, M., 2020. Pyrolysis of biological wastes for bioenergy production: Thermo-kinetic studies with machine-learning method and Py-GC/MS analysis. Fuel, 269, 117238.

Tedetti, M., Cuet, P., Guigue, C., Goutx, M., 2011. Characterization of dissolved organic matter in a coral reef ecosystem subjected to anthropogenic pressures using multi-dimensional fluorescence spectroscopy. Sci. Total Environ. 409, 2198-2210.

Tang, Y., Li, X., Dong, B., Huang, J., Wei, Y., Dai, X., Dai, L., 2018. Effect of aromatic repolymerization of humic acid-like fraction on digestate phytotoxicity reduction during high-solid anaerobic digestion for stabilization treatment of sewage sludge. Water Res. 143, 436-444.

Tang, Y., Dai, X., Dong, B., Guo, Y., Dai, L., 2020. Humification in extracellular polymeric substances (EPS) dominates methane release and EPS reconstruction during the sludge stabilization of high-solid anaerobic digestion. Water Res. 175, 115686.

686 Tan, K. H., 2014. Humic matter in soil and the environment: Principles and controversies.
687 CRC Press.
688 Tan, W., Xi, B., Wang, G., Jie, J., He, X., Mao, X., Gao, R., Huang, C., Zhang, H., Li, D., Jia,
689 Y., Yuan, Y., Zhao, X., 2017. Increased electron-accepting and decreased electron
690 donating capacities of soil humic substances in response to increasing temperature.
691 Environ. Sci. Technol. 51, 3176–3186.
692 Wu, J. O., Zhao, Y., Zhao, W., Yang, T. X., Zhang, X., Xie, X. Y., Cui, H. Y., Wei, Z. M., 2017.
693 Effect of precursors combined with bacteria communities on the formation of
694 humic substances during different materials composting. Bioresour. Technol. 226,
695 191-199.
696 Weishaar, J. L., Aiken, G. R., Bergamaschi, B. A., Fram, M. S., Fujii, R., Mopper, K., 2003.
697 Evaluation of specific ultraviolet absorbance as an indicator of the chemical
698 composition and reactivity of dissolved organic carbon. Environ. Sci. Technol. 37
699 (20), 4702-4708.
700 Wang, X., Muhmood, A., Dong, R., Wu, S., 2020. Synthesis of humic-like acid from
701 biomass pretreatment liquor: Quantitative appraisal of electron transferring
702 capacity and metal-binding potential. J. Clean. Prod. 255,120243.
703 Wang, M., Zhao, Z., Zhang, Y., 2019. Disposal of Fenton sludge with anaerobic digestion
704 and the roles of humic acids involved in Fenton sludge, Water Res. 163, 114900.
705 Xu, H., Li, Y., Hua, D., Zhao, Y., Mu, H., Chen, H., Chen, G. 2020. Enhancing the anaerobic
706 digestion of corn stover by chemical pretreatment with the black liquor from the
707 paper industry. Bioresour. Technol. 306, 123090.
708 Yap, S. D., Astals, S., Lu, Y., Peces, M., Jensen, P. D., Batstone, D. J., Tait, S., 2018. Humic
709 acid inhibition of hydrolysis and methanogenesis with different anaerobic inocula.
710 Waste Manage. 80, 130-136.
711 Yap, S. D., Astals, S., Jensen, P. D., Batstone, D. J., Tait, S., 2017. Indigenous microbial
712 capability in solid manure residues to start-up solid-phase anaerobic digesters.
713 Waste Manage. 64, 79-87.
714 Yang, F., Zhang, S., Cheng, K., Antonietti, M., 2019. A hydrothermal process to turn waste
715 biomass into artificial fulvic and humic acids for soil remediation. Sci. Total Environ.
716 686, 1140-1151.
717 Zhang, W., Wei, Q., Wu, S., Qi, D., Li, W., Zuo, Z., Dong, R., 2014. Batch anaerobic co-
718 digestion of pig manure with dewatered sewage sludge under mesophilic
719 conditions. Appl. Energ. 128, 175-183.
720 Zhao, X., Tan, W., Peng, J., Dang, Q., Zhang, H., Xi, B., 2020. Biowaste-source-dependent
721 synthetic pathways of redox functional groups within humic acids favoring
722 pentachlorophenol dichlorination in composting process. Environ. Intern. 135,
723 105380.

724 Zhou, Y., Selvam, A., Wong, J. W. C., 2014. Evaluation of humic substances during co-
725 composting of food waste, sawdust and Chinese medicinal herbal residues.
726 Bioresour. Technol. 168, 229-234.
727 Zhang, Y. C., Yue, B. D., Ma, H., 2015. Darkening mechanism and kinetics of humification
728 process in catechol-Maillard system. Chemosphere, 130, 40−45.
729

Mechanisms of genuine humic acid evolution and its dynamic interaction with methane production in anaerobic digestion processes

Wang, Xiqing

2020-10-14

Wang X, Muhmood A, Lyu T, et al., (2021) Mechanisms of genuine humic acid evolution and its dynamic interaction with methane production in anaerobic digestion processes. Chemical Engineering Journal, Volume 408, March 2021, Article number 127322

https://doi.org/10.1016/j.cej.2020.127322